Article:
Seilert, J. orcid.org/0000-0002-0149-7253, Rappolt, M. orcid.org/0000-0001-9942-3035, Dol, G. et al. (1 more author) (2024) Interplay of Polymorphic Transition and Mixed Crystal Formation in Model Fat Systems. Crystal Growth and Design, 24 (3). pp. 1146-1158. ISSN 1528-7483

https://doi.org/10.1021/acs.cgd.3c01164

Supporting Information

Interplay of polymorphic transition and mixed crystal formation in model fat systems

Julia Seilert[1*], *Michael Rappolt*[2], *Georg Dol*[3], *Eckhard Flöter*[1]

[1] Department of Food Process Engineering, Technische Universität Berlin, Straße des 17. Juni 135, Berlin 10623, Germany

[2] School of Food Science and Nutrition, Food Colloids and Bioprocessing Group, University of Leeds, Leeds LS2 9JT, U.K.

[3] Upfield Research & Development B.V., Food Science Centre, Bronland 18, 6708 WH Wageningen, The Netherlands

Content:

1. SAXS/WAXS pattern: liquid fraction subtraction

2. Analysis of the first order peak

3. Indexing of diffraction pattern (2L-stacking).

4. Literature data on short and long spacings of some triglycerides

5. Triglyceride composition determined from fatty acid profile

***Correspondence:** Department of Food Process Engineering, Technische Universität Berlin, Straße des 17. Juni 135, Berlin 10623, Germany; Email: julia.seilert@tu-berlin.de

1. SAXS/WAXS pattern: liquid fraction subtraction

From all pattern, the liquid contribution of the molten sample was subtracted. Therefore, the scattering contribution from molten triglycerides obtained after 10 min at 70 °C was used. The subtraction was performed as follows:

$$I^*_{sample} = I_{sample} - I_{molten} \cdot \frac{\sum_{q=10}^{11} I_{sample}}{\sum_{q=10}^{11} I_{molten}},$$

with I^*_{sample} being the signal intensity corrected for the liquid contribution, and I_{molten} denoting the signal intensity obtained for the molten sample. Only data points between 10 and 11 nm^{-1} were used, where exclusively the molten phase contributes to the scattering pattern. **Figure S1** gives an overview of the data before and after liquid subtraction.

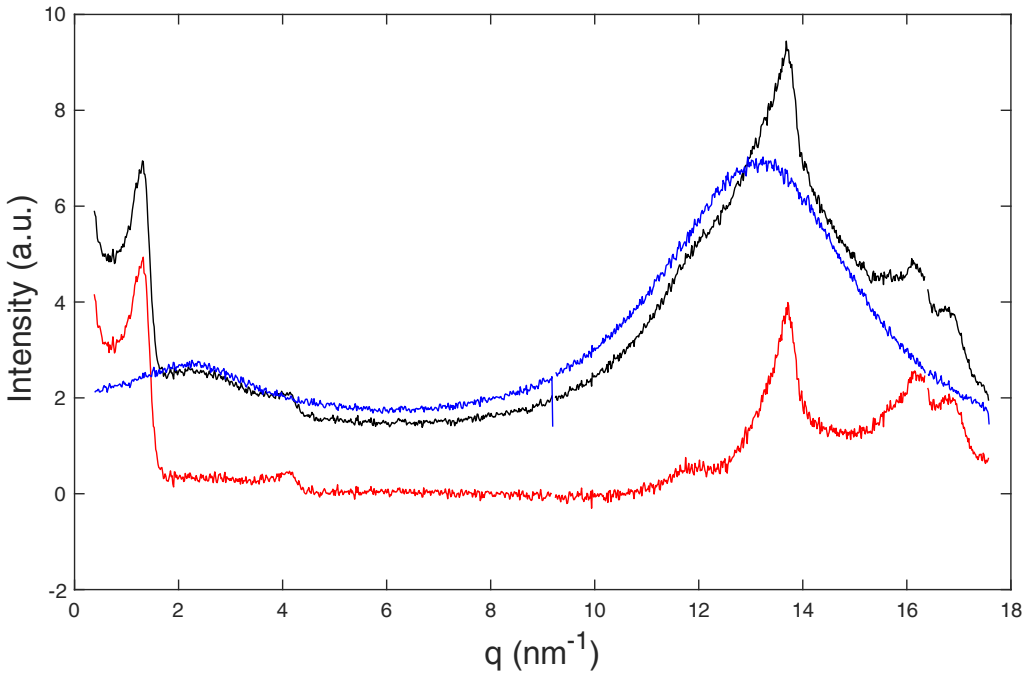

Figure S1. SAXS/WAXS pattern of H3.3 crystallized with a cooling rate of 5 °C/min. Raw data (black), signal of the molten sample at 70 °C (blue), data after subtraction of the liquid scattering contribution (red) as normalized in the q interval from 10 to 11 nm^{-1}.

2. Analysis of the first order peak

Peak analysis of the 1st order reflection (001) in the SAXS region, including determining the area was performed using MATLAB2020b, see **Figure S2**. The raw data were smoothed, using a moving average filter. After that, the numerical maximum position was determined. This peak position determination was further refined. In order to find a more accurate maximum position, a polynomial fit of the smoothed data was performed in a relatively narrow and asymmetrical window (see blue curve fit). An asymmetrical window was used to account for the peak smearing due to the line collimation focus of the instrument. A 3rd degree polynomial was fitted in the window. Initial tests proved a window of -11 and +5 data points around the numerical maximum to be sufficient. The maximum of the polynomial fit was considered the true maximum position from which the d-spacing (long spacing) was calculated. Best absolute d-values were additionally cross-checking in the pure phase regime, using the reflections at h = 0, 1, 3, see **Figure S3**.

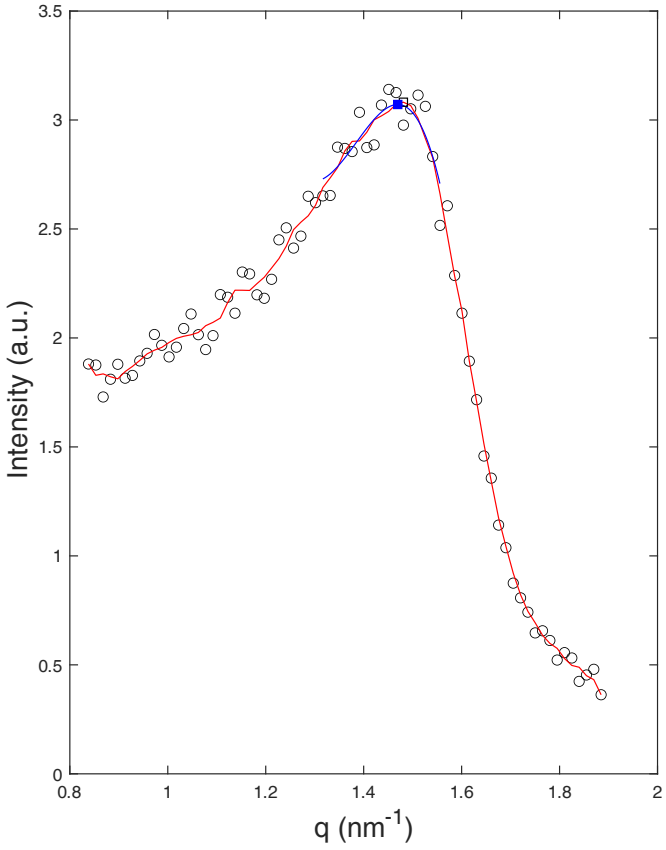

Figure S2. Exemplary peak fit analysis performed in MATLAB2020b on SAXS data obtained for H3.3 crystallized at a cooling rate of 5 °C/min. Raw data (hollow circles) were smoothed via moving average filter (number of data points = 5) (red line). The numerical peak maximum position (hollow square), 3rd degree polynomial fit around the numerical maximum position in a data range of –11 and +5 data points (blue line) and the true peak maximum position (solid blue circle) are shown.

3. Indexing of diffraction pattern (2L-stacking)

Best absolute d-values were additionally cross-checked in the pure phase regime (α and β) at h = 0, 1, 3 for H3.3 crystallized at 5 °C/min, which gives a more precise absolute d-spacing determination. Note, all d-spacings obtained from the 1st order reflection only were therefore corrected with an offset of -2 Å.

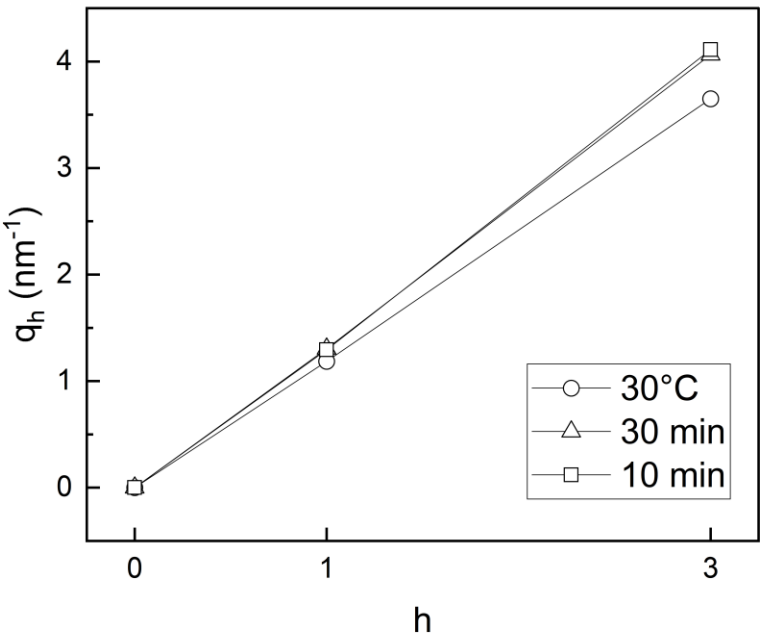

Figure S3. Indexing of the diffraction pattern in the SAXS regime. Linear fits of recorded 1st and 3rd order reflection position, q_h, as a function of the Miller index h were used for calculating most accurate absolute d-spacings. Note, the slopes of the linear fit give the d-values in pure phase regime (α at 30 °C in the cooling step, β at 10 and 30 min isothermal holding time at 25 °C recorded for H3.3 cooled at 5 K °C/min).

4. Literature data on short and long spacings of some triglycerides

The literature data are used as reference data to identify the polymorphic forms of the TG crystals examined in the study.

Table S1. Short spacings of triglycerides in various polymorphs reported in the literature. Spacing are given in units of Å.

TAG	α	β'	β	Ref.
SSS	4.15	4.2, 3.8	4.6, 3.9, 3.7	[1]
	4.1-4.2	4.2, 3.8	4.6, 3.7, 3.85	[2]
PPP	4.15		4.6, 3.85, 3.7	[3]
PSS	4.11	4.19, 3.81	4.52, 3.83, 3.65	[4]
PSP	4.13	4.33, 4.2, 4.03, 3.83		[5,6]
*PPMy**	4.13	4.36, 4.19, 3.99, 3.8		[7]
*PPLa**	4.14	4.39, 4.23, 4.03, 3.83	5.47, 4.71, 4.57, 3.9, 3.74	[7]

*Short spacing of β'_1

Table S2. Long spacings of triglycerides in various polymorphs reported in the literature, units in Å.

TAG	α	β'	β	Ref.
MyMyMy	41.2	37.65	35.8	[8]
PPP	45.6	42.3	40.6	[8]
SSS	50.6	46.8	45	[8]
PPMy	45.3	40.5	40	[7]
PPLa	43.3	39	40.9	[7]

5. Triglyceride composition determined from fatty acid profile

The triglycerides composition was determined for FHRO, the structuring agent of the H3 system, from the fatty acid profile (**Table 1**) according to Coleman[9]. Here, unsaturated fatty acids are assumed to be preferably on the sn_2 position, all other fatty acids are randomly distributed over sn_1 and sn_3. This results in a tristearin (SSS) content of 72.3 %, and SS-X/X-SS/S-X-S, with X being any fatty acid that is not stearic acid, to be 25.5 %. In total, saturated stearic-dominated triglycerides make up approx. 97.8 %.

The triglyceride composition for the blend of commercial hardstocks for the H3+H2M system was determined from the fatty acid profile (**Table 1**) assuming random distribution of the fatty acids over the glycerol backbones which complies with chemical interesterification. That the respective enzymatic interesterification reached this equilibrium state was verified by the sn_2 fatty acid profile from the supplier.

Table S3. Triglyceride composition of the H3 and H2M melting groups of the structuring system for the H3+H2M blends based on a blend of commercial hardstocks. The composition was determined on the basis of the fatty acid composition.

TAG group	TAG	%
H3	SSS	2.0
	PPP	1.3
	PPS	4.5
	SSP	5.1
H2M	SSLa	6.8
	SSMy	2.1
	PPLa	5.1
	PPMy	1.6
	SPLa	3.7
	SPMy	11.8

Mixed triglycerides also include enantiomers and the (a)symmetrical counterparts, e.g., the amount of PPS also includes the amount of PSP and SPP. For triglycerides composed of three fatty acids (ABC), six arrangements over the glycerol backbone have to be taken into account.

References

(1) Oh, J.-H.; McCurdy, A. R.; Clark, S.; Swanson, B. G. Characterization and Thermal Stability of Polymorphic Forms of Synthesized Tristearin. *J Food Science* **2002**, *67* (8), 2911–2917. DOI: 10.1111/j.1365-2621.2002.tb08837.x.

(2) Lavigne, F.; Bourgaux, C.; Ollivon, M. Phase transitions of saturated triglycerides. *J. Phys. IV France* **1993**, *03* (C8), C8-137-C8-140. DOI: 10.1051/jp4:1993825.

(3) Sato, K.; Ueno, S.; Yano, J. Molecular interactions and kinetic properties of fats. *Progress in lipid research* **1999**, *38*, 91–116.

(4) Bouzidi, L.; Narine, S. S. Relationships between molecular structure and kinetic and thermodynamic controls in lipid systems. Part II: Phase behavior and transformation paths of SSS, PSS and PPS saturated triacylglycerols—Effect of chain length mismatch. *Chemistry and Physics of Lipids* **2012**, *165* (1), 77–88. DOI: 10.1016/j.chemphyslip.2011.11.005.

(5) Bhaggan, K.; Smith, K. W.; Blecker, C.; Danthine, S. Binary Mixtures of Tripalmitoylglycerol (PPP) and 1,3-Dipalmitoyl-2-stearoyl- sn -glycerol (PSP): Polymorphism and Kinetic Phase Behavior. *Eur. J. Lipid Sci. Technol.* **2018**, *120* (3), 1700306. DOI: 10.1002/ejlt.201700306.

(6) Bhaggan, K.; Smith, K. W.; Blecker, C.; Danthine, S. Polymorphism and Kinetic Behavior of Binary Mixtures of Trisaturated Triacylglycerols Containing Palmitic and Stearic Acid Under Non-Isothermal Conditions. *Eur. J. Lipid Sci. Technol.* **2018**, *120* (9), 1800072. DOI: 10.1002/ejlt.201800072.

(7) Kodali, D. R.; Atkinson, D.; Small, D. M. Polymorphic behavior of 1,2-dipalmitoyl-3-lauroyl(PP12)- and 3-myristoyl(PP14)-sn-glycerols. *Journal of Lipid Research* **1990**, *31*.

(8) Lutton, E. S. Triple Chain-Length Structures of Saturated Triglycerides. *J. Am. Chem. Soc* **1948**, *70* (1), 248–254.

(9) Coleman, M. H. The Unsolved Problems of Triglyceride Analysis. *J Am Oil Chem Soc* **1965**, *42*.